Microscopic model for non-excitonic mechanism of 1.5 μm photoluminescence of the Er3+ ion in crystalline Si

Forcales Fernandez, M.; Gregorkiewicz, T.; Bresler, M.S.; Gusev, O.B.; Bradley, I.V.; Wells, J.P.

Publication date
2003

Published in
Physical Review B

Microscopic model for nonexcitonic mechanism of 1.5-μm photoluminescence of the Er^{3+} ion in crystalline Si

M. Forcales and T. Gregorkiewicz
Van der Waals–Zeeman Institute, University of Amsterdam, Valckenierstraat 65, NL-1018 XE Amsterdam, The Netherlands

M. S. Bresler and O. B. Gusev
A. F. Ioffe Physicotechnical Institute, Russian Academy of Sciences, 194021 St. Petersburg, Russia

I. V. Bradley and J-P. R. Wells
FOM Institute for Plasma Physics "Rijnhuizen," P.O. Box 1207, NL-3430 BE Nieuwegein, The Netherlands and Department of Physics, Heriot Watt University, Edinburgh EH14 4AS, United Kingdom

(Received 26 April 2002; revised manuscript received 17 September 2002; published 4 February 2003)

Excitation mechanisms of Er^{3+} ion in crystalline silicon, responsible for the photoluminescence at $\lambda \approx 1.54$ μm, are reexamined in view of the new information revealed for this system by two-color spectroscopy in the visible and the midinfrared. We argue that the appearance of the midinfrared induced emission from the $^4I_{13/2}$ excited state of Er^{3+} and the recently identified afterglow effect represent characteristic fingerprints of a specific and so far unrecognized excitation path, different from the usually considered exciton-mediated energy transfer. We propose a microscopic model of this mechanism, where excitation of Er^{3+} is accomplished in two distinct steps: electron localization at an Er-related donor level and its subsequent recombination with a hole. These two stages can be separated in time, leading to a situation when the appearance of Er photoluminescence is controlled by availability of one carrier type only. We propose a set of rate equations to describe this process and show that the experimental data are well accounted for. Further, we consider potential of the nonexcitonic mechanism for realization of efficient temperature-stable emission from Er-doped crystalline silicon.

DOI: 10.1103/PhysRevB.67.085303 PACS number(s): 78.66.Db, 61.72.Tt, 41.60.Cr

I. INTRODUCTION

In spite of the obvious natural disadvantage of a relatively small and indirect band gap, silicon enjoys a renewed interest as material for optoelectronic and photonic applications. In particular, encouraging results have recently been reported for silicon-derived materials such as silicon nanocrystals dispersed in SiO_2 matrix,[1] and SiO_2 codoped with silicon nanocrystals and Er^{3+}.[2] Intense room-temperature emission has been obtained upon the formation of boron inclusions in crystalline silicon (c-Si) by implantation.[3] Parallel to these new concepts, research on optical doping with transition-metal elements as a way to improve optical activity of c-Si is set forth. Emission from rare-earth (RE) ions is characterized by a temperature-stable wavelength and a narrow linewidth. Here Er doping is most intensively investigated. When silicon is doped with erbium, light emission due to the $^4I_{13/2} \rightarrow {}^4I_{15/2}$ intra-4f-electron shell transition can be observed at $\lambda_{Er} \approx 1.54$ μm. This wavelength falls in the range of minimum losses of silica-based optical fibers used in telecommunications. Being fully compatible with the standard VLSI silicon technology, development of Si:Er structures by ion implantation is especially interesting. Unfortunately, the intensity of electroluminescence and photoluminescence (PL) from RE-doped semiconductors reduces strongly upon temperature increase. Consequently, intense room-temperature emission from devices based on c-Si:Er remains yet to be demonstrated. It is generally believed that proper engineering and optimization of the energy transfer between silicon host and Er^{3+} ion constitutes the key to the realization of this goal. Ideally, the excitation process of the energy transfer into the RE ion core should be very efficient, while the reversal of this process, usually termed as *back transfer*, needs to be suppressed. Also other nonradiative deexcitation channels of excited Er^{3+} ions must be eliminated. In the past, excitation mechanism of Er^{3+} ions in crystalline Si has been modeled theoretically,[4,5] and the recombination of an electron-hole pair or impact with a hot carrier (reverse biased diodes) have been postulated to be responsible for the excitation of Er^{3+} ions in crystalline Si. Under optical pumping by photons with energies larger than that of the silicon band gap, electrons and holes are generated in conduction and valence bands, respectively. The carriers recombine in an Auger process transferring the energy to the 4f-electron shell of the Er^{3+} ion. As a result of this excitation, characteristic emission due to the $^4I_{13/2} \rightarrow {}^4I_{15/2}$ transition ($E_{4f} \approx 800$ meV) appears with a decay constant of $\tau_1 \approx 1$ ms.[6–8] The higher excited states are not directly available since their energies exceed the silicon band-gap value ($E_G \approx 1170$ meV at $T = 4.2$ K compared to 1240 meV necessary for excitation into the $^4I_{11/2}$ second excited state of Er^{3+} ion). A model involving recombination of an exciton bound to an Er-related donor was proposed.[9] In this case, the major part of the electron-hole recombination energy is used for the 4f-electron shell excitation and the excess energy is released by the excitation of the electron from the erbium-related donor level into the band. While such an energy-transfer channel can be efficient, it requires high electron and hole concentrations for exciton generation. This, in turn, leads to deexcitation of Er^{3+} ions due to Auger interaction with free

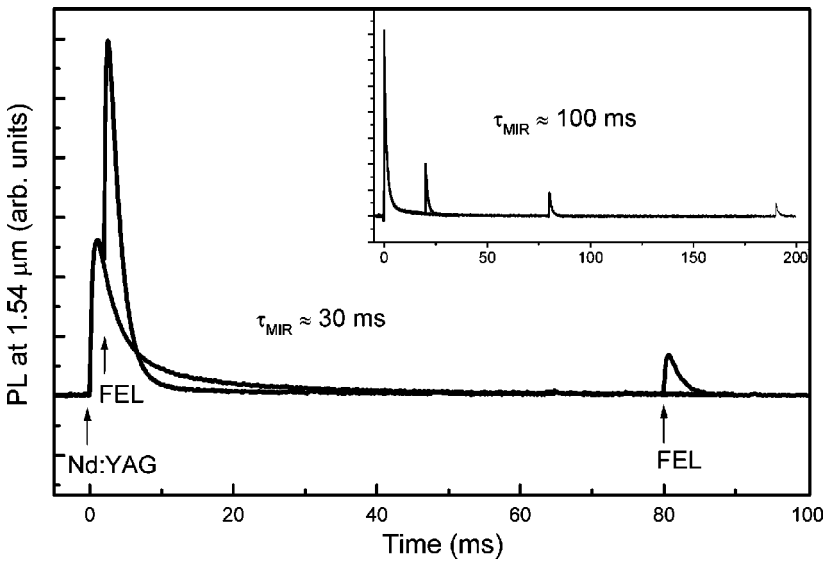

FIG. 1. Low-temperature ($T=4.2$ K) dynamics of Er-related PL signal at $\lambda\approx1.54$ μm. The pump excitation density was kept low to avoid saturation. MIR pulse with $\lambda_{FEL}\approx10$ μm was applied with a delay Δt of 2 and 80 ms. The enhancement of Er PL is characterized by a decay time $\tau_{MIR}\approx30$ ms. In the inset, the MIR-induced enhancement ($\Delta t=20,80,170$ ms) is shown for a sample characterized by an extremely long time constant of $\tau_{MIR}\approx100$ ms.

carriers. Under these circumstances, the experimentally observed saturation of Er PL for high excitation densities can be caused by a limited concentration of optically active Er^{3+} ions or, alternatively, can result from a competition between excitation and Auger deexcitation processes.

Experimental evidence used thus far for modeling of Er excitation process came almost exclusively from investigations of temperature variations of intensity and lifetime of the Er-related luminescence. Unfortunately, thermal activation is rather indiscriminate: different effects appear simultaneously and become entangled. Consequently, detailed identification of individual processes is difficult and the proposed models of Si:Er excitation mechanism remain rather speculative.

The situation is much more favorable when midinfrared (MIR) laser light rather than temperature is used for selectively activate specific energy transfers. In that case individual stages of excitation and deexcitation processes can be selectively addressed by wavelength tuning. Indeed, new information on Si:Er emission mechanism has been obtained using two-color spectroscopy in the visible and the MIR ranges.[10] In particular, it was shown that a MIR laser pulse applied shortly after band-to-band (pulsed) excitation leads to an additional emission from Er^{3+} ions.[11] Temporary storage of nonequilibrium carriers at traps available in the host was found to be responsible for the effect.[12] More recently, we pointed out that the thermal release of carriers stored at these traps gives rise to a slowly decaying component of Er PL, *the afterglow*. In a dedicated study,[13] we have explicitly shown that the MIR-induced excitation of Er and the afterglow effects are mutually related, and proposed mathematical description relating amplitudes and temporal characteristics of both effects.

In the current contribution, we reexamine the excitation mechanism of Si:Er in view of the novel information revealed by two-color MIR spectroscopy. In addition to the already published data,[13] we build on a careful investigation of the magnitude of the MIR-induced Er PL on the MIR photon flux. We propose a microscopic model for the excitation process, in which the FEL pulse releases holes stored at acceptor (or acceptorlike) traps, which subsequently recombine with electrons localized at an Er-related donor level. Such a process is distinctly different from the exciton-related energy transfer commonly considered for Er in crystalline silicon matrix and dominant upon (high-power) band-to-band excitation. Following this scheme, we develop a set of rate equations to describe the relevant physical mechanisms. We show that the experimental results can be satisfactorily simulated using the proposed description. Finally, we consider whether this sequential excitation path could be utilized for the increase of thermal stability of emission from *c*-Si:Er.

II. EXPERIMENTAL DETAILS

As reported in our preceding study,[13] the MIR-induced Er PL (uniquely related to the afterglow effect of slowly decaying emission) is omnipresent for *c*-Si:Er. It is best revealed under low pumping density of band-to-band excitation, when its magnitude is much larger than that of the exciton-mediated Er^{3+} emission. Our investigations show that, while the characteristics of the MIR-induced Er PL depend on sample parameters, the effect is stronger when Er is implanted into *p*- than into *n*-type substrates. Consequently, for the use in the present study a set of several Si:Er samples were prepared from Czochralski-grown *p*-type boron-doped silicon with room-temperature resistivity of 5–10 Ωcm. All these data presented in this paper (with an exception of the spectrum shown in the inset of Fig. 1) have been obtained for a particular sample implanted with 300-keV Er ions to a dose of 3×10^{12} cm^{-2}. The concentration of erbium in the implanted layer was around 10^{19} cm^{-3}. The sample was coimplanted with oxygen ions with an energy of 40 keV and to a concentration comparable to that of erbium ions. Oxygen codoping is known to increase the intensity of Er PL and to reduce its thermal quenching. Implantations were followed by 900 °C annealing during 30 m.

Two-color photoluminescence experiments have been performed with the primary pulsed excitation by the second harmonic of a Nd:YAG laser (532 nm) and the secondary

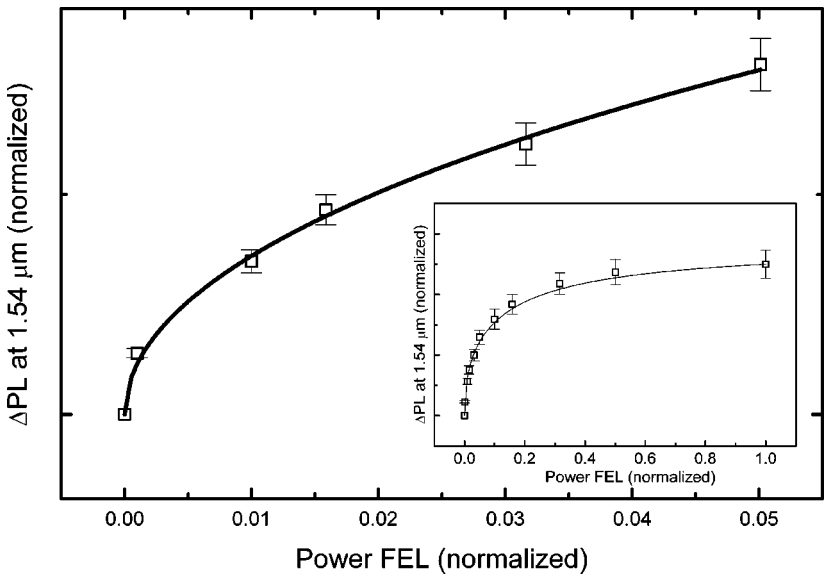

FIG. 2. Low-energy range excitation density dependence (FEL) of the MIR-induced $\lambda \approx 1.54$-μm Er emission, measured for a low-level band-to-band pumping, for $\lambda_{FEL} \approx 10$ μm and $\Delta t = 5$ ms. The inset shows the dependence for the full available FEL power range. The solid lines are simulations based on Eq. (27).

excitation with MIR radiation from a free-electron laser (FEL). All results were obtained at $T = 4.2$ K. A detailed description of experimental procedures can be found in our previous report.[13] In these experiments, intensity of the $\lambda \approx 1.54$ μm emission related to the transition from the $^4I_{13/2}$ excited state to the $^4I_{15/2}$ ground state of Er^{3+} ion was investigated as a function of primary and secondary excitation densities.

III. EXPERIMENTAL RESULTS

Building upon the earlier experience,[13] the present experiments were performed under low pumping density of the Nd:YAG laser. Figure 1 illustrates the MIR-induced Er PL for the sample used in the current study; a strong response of Er^{3+}-related emission at $\lambda_{Er} \approx 1.54$ μm can be seen in a situation when the MIR pulse from FEL (photon energy $\sim$120 meV, power $\sim$10 mW/cm^2) was fired with delay times of $\Delta t = 2$ ms and $\Delta t = 80$ ms with respect to the band-to-band excitation with Nd:YAG laser (power density of 10 μJ/cm^2, duration $\sim$100 ps). The PL signal dynamics were recorded with a Ge detector. For this sample, decay time of the MIR-induced enhancement of $\tau_{MIR} \approx 30$ ms has been concluded. The particular value of this time constant depends on sample characteristics. For comparison, an extreme example is shown in the inset of Fig. 1. In this case, the FEL-induced Er^{3+}-related emission can be observed even for very large delay times of $\Delta t = 170$ ms and a very long decay time of the MIR-induced effect of $\tau_{MIR} \approx 100$ ms has been concluded.

In Fig. 2, we show the results of a detailed investigation of the magnitude of the MIR-induced Er PL enhancement on FEL photon flux, measured at a fixed low level of band-to-band excitation. The experiment is realized by reducing the FEL pulse energy with a set of internal attenuators. We pay special attention to the lowest levels of FEL power, at which the enhancement effect can still be detected. The results illustrated in Fig. 2 were taken for a fixed delay time of $\Delta t = 5$ ms and for the MIR photon energy of $\sim$120 meV, but similar characteristics are found also for other values of delay time and FEL photon energy. The amplitude of the MIR-induced PL enhancement shows clearly a sublinear behavior. The complete dependence, for the full available range of FEL power, is shown in the inset of Fig. 2. As can be concluded, the effect saturates in agreement with the model relating it to trap ionization.[11]

Finally, in Fig. 3 magnitudes of the MIR- and Nd:YAG-induced Er PL signals are shown as a function of the visible pump density. As explained earlier, in order to avoid saturation in the current measurements we used low-energy range of Nd:YAG laser pulses. The FEL (photon energy $\sim$90 meV, power fixed at a maximum level of $\sim$200 mW/cm^2) is fired with a delay of $\Delta t = 3$ ms. As can be seen, an increase of the visible pump-induced signal (i) coincides with the saturation of the Er PL enhancement appearing upon FEL pulse (ii).

IV. DISCUSSION

A. Comparison of previous excitation models with experimental results

As explained in the Introduction, the available excitation models of Si:Er PL involve simultaneous generation of electrons and holes. Since these are characterized by short lifetimes (microsecond range at cryogenic temperatures), they cannot be accountable for the most characteristic feature of the MIR-induced excitation process illustrated in Fig. 1, namely, the occurrence of the PL enhancement after long delay times (hundreds of ms). In order to identify the microscopic physical mechanism responsible for the FEL-induced excitation of Er ions, we recall that next to phonon generation (due to multiphonon absorption), ionization of shallow traps is the most important effect induced by MIR radiation in a semiconductor matrix. Indeed, in the past we have shown that Er emission appearing upon the application of the MIR pulse can be related to the optical ionization of traps filled by the pump pulse of the visible laser.[11,13] In what follows, we will pursue to work out details of that process.

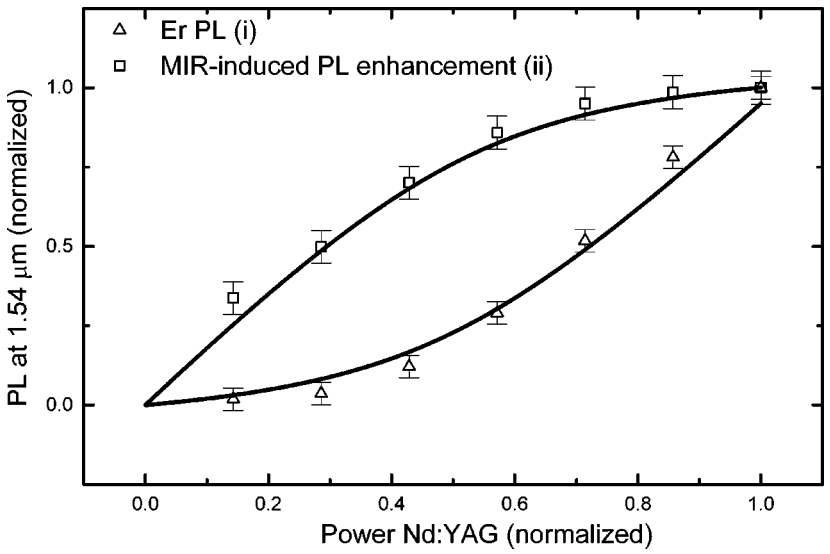

FIG. 3. Excitation density dependence (Nd:YAG) of the $\lambda \approx 1.54$-μm Er emission induced by (i) Nd:YAG (band-to-band) and (ii) FEL (MIR) laser pulses: Amplitude of (i) increases stronger as saturation of (ii) sets in. The MIR pulse at $\lambda_{FEL} \approx 13.5$ μm (constant power) is applied with a delay of $\Delta t = 3$ ms. The Nd:YAG power is normalized to the value at which the amplitude of the FEL-induced Er PL signal saturates. The solid lines are simulated from Eqs. (28) and (29).

Since the recombination of an electron-hole pair is necessary for excitation of the $4f$-electron core of an Er^{3+} ion, we will first consider whether the additional Er-related PL could appear due to the release of excitons stored in the system. We assume, see Fig. 4(a), that following a band-to-band pump pulse, excitation of Er^{3+} ions takes place by recombination of an exciton bound to an Er-related level. Upon the band-to-band pump pulse, it is reasonable to consider localization of excitons also at centers [e.g., donors—see Fig. 4(a)] not related to Er. When FEL is fired, the absorption of the MIR radiation could remove electrons (labeled as 1) from the impurity levels, thus releasing excitons. Free excitons (labeled as 2) could then be captured by Er-related centers, leading to Er^{3+} excitation and the enhancement of PL signal. However, as illustrated in Fig. 1, the MIR-induced enhancement can appear with a time constant exceeding $\tau_{MIR} > 100$ ms, i.e., two orders of magnitude longer than the reported lifetimes of bound excitons in silicon (exciton binding at isoelectronic centers), ruling over this possibility.

Consequently, we will now consider a different mechanism, see Fig. 4(b). In this excitation model, in contrast to the previous one, we introduce both electrons and holes bound at donor and acceptor impurities, respectively. In that case we could imagine that the acceptor levels would originate from Si material rather than being related to the Er doping. The investigated samples were prepared from *p*-type (boron-doped) Si substrate, and although the concentration of acceptors in the Er implanted layer is several orders of magnitude lower than that of Er, it is reasonable to include them here, as they are available within the bulk of the material that is penetrated by the MIR beam. When the MIR radiation is applied, ionization of both types of trapping levels will take place. Their subsequent recombination (at the Er-related center) could lead to an additional excitation of Er^{3+}. However, under these circumstances the amplitude of the MIR-induced Er PL enhancement should be proportional to $(I_{FEL})^2$, as two photons (for ionization of two carriers of the opposite type) are necessary for the excitation of an Er^{3+} ion. While in practice both ionization processes could have different probability leading to deviations from quadratic dependence, the experimental data in Fig. 2 clearly show a sublinear character, even for the lowest power range. behavior Such a cannot be explained by the considered mechanism and suggests a different, thus far unrecognized, excitation path.

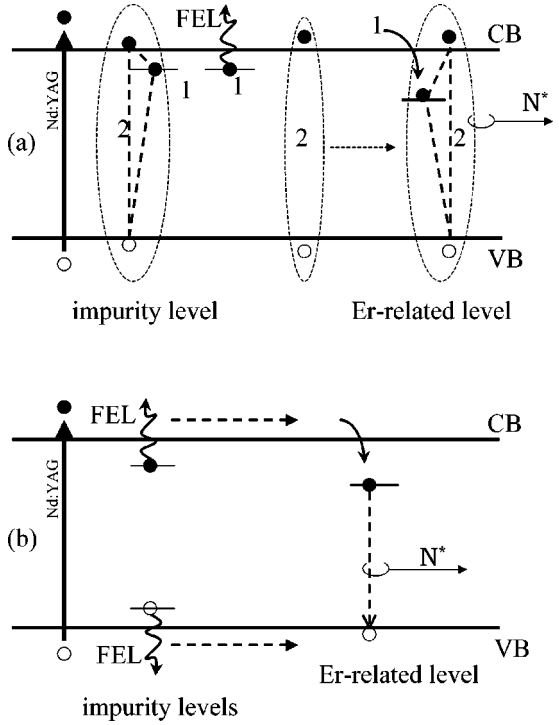

FIG. 4. Illustration of possible MIR-induced excitations of Er by the release of (a) excitons and (b) two carriers of opposite type—see text for a discussion.

B. Microscopic model of sequential excitation

1. Slow excitation mechanism

In order to account for our experimental results, we propose a mechanism in which the excitation of an Er^{3+} ion is achieved by the recombination of a hole with an electron

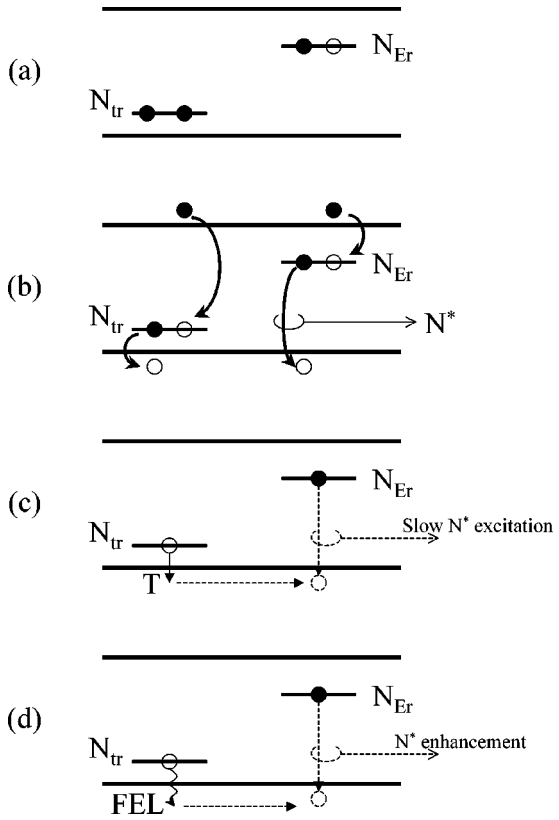

FIG. 5. Illustration of the proposed sequential mechanism for Er excitation—see text for the full description.

localized at an Er-related level. The assumption is based on multiple reports on donor generation upon Er implantation in oxygen-rich Si,[14,15] and on our own observation that the MIR-induced Er PL is more pronounced on samples prepared on *p*- than *n*-type substrates. In that way the excitation process can be divided into two steps: localization of an electron and subsequent capture of a free hole from the valence band. What distinguishes this mechanism from these usually considered one is the stable character of the ''intermediate'' stage when an electron is present at the Er-related level while a free hole is not available to complete the excitation process.

The proposed mechanism is schematically depicted in Fig. 5. Following the above sketched scenario, we consider two different impurity levels. A donor level related to erbium implantation, with N_{Er}, as the total concentration of optically active erbium ions, and an acceptor level related to the Si substrate (p type), with N_{tr}, as the total concentration of hole traps. Initially, when the system is in thermal equilibrium at low temperature ($T=4.2$ K), impurity traps will be filled with electrons and erbium donor centers will be partially filled with electrons if the Fermi level is close to this level, see Fig. 5(a). After band-to-band excitation by the Nd:YAG ($I\delta(t-t_0)$ being the intensity of the visible excitation in a delta-shape pulse), free carriers are created. If we define f and f' as the electron filling factors of acceptor traps and erbium-related donor levels, respectively, then the situation can be described by the following rate equations:

$$\frac{dn}{dt}=\alpha I\delta(t-t_0)-rnp-C_{tr}nN_{tr}(1-f)-C_{d\mathrm{Er}}nN_{\mathrm{Er}}(1-f')+rn_0p_0+C_{tr}n_0\frac{(1-f_0)}{f_0}N_{tr}f+C_{d\mathrm{Er}}n_0\frac{(1-f_0')}{f_0'}N_{\mathrm{Er}}f', \tag{1}$$

$$\frac{dp}{dt}=\alpha I\delta(t-t_0)-rnp-C_{ptr}pN_{tr}f-C_ApN_{\mathrm{Er}}f'+rn_0p_0+C_{ptr}p_0\frac{f_0}{(1-f_0)}N_{tr}(1-f)+C_Ap_0\frac{f_0'}{(1-f_0')}N_{\mathrm{Er}}(1-f'), \tag{2}$$

$$N_{tr}\frac{df}{dt}=C_{tr}nN_{tr}(1-f)-C_{ptr}pN_{tr}f-C_{tr}n_0\frac{(1-f_0)}{f_0}N_{tr}f+C_{ptr}p_0\frac{f_0}{(1-f_0)}N_{tr}(1-f), \tag{3}$$

$$N_{\mathrm{Er}}\frac{df'}{dt}=C_{d\mathrm{Er}}nN_{\mathrm{Er}}(1-f')-C_ApN_{\mathrm{Er}}f'-C_{d\mathrm{Er}}n_0\frac{(1-f_0')}{f_0'}N_{\mathrm{Er}}f'+C_Ap_0\frac{f_0'}{(1-f_0')}N_{\mathrm{Er}}(1-f'), \tag{4}$$

$$\frac{dN^*}{dt}=C_Apf'(N_{\mathrm{Er}}-N^*)-\frac{N^*}{\tau}. \tag{5}$$

Here n and p are the concentrations of free electrons and holes, N^* is the concentration of excited erbium ions, α, r are the band-to-band absorption and recombination coefficients, respectively. C_{tr}, $C_{d\mathrm{Er}}$, C_{ptr}, and C_A are the capture coefficients of electrons and holes by traps and erbium centers, respectively. The rate equations written above describe the most general dynamic process of free carrier capture at acceptors and donors, and also the reverse process (thermal effects) of carrier release. The coefficients of the reverse processes were found using detailed balance principle in equilibrium conditions. Note that the quantities n_0, p_0, f_0, and f_0' depend exponentially on the temperature. In order to solve this nonlinear rate equation system and obtain analytical expressions, we introduce artificially three different time regimes. In the first one, we consider only very fast processes. We will ignore capture process to impurities and we only take into account the recombination of free charges. In the second one, we ignore reverse processes (as the thermal emission is very slow at $T=4.2$ K); in that way we can find the evolution of the filling factors f and f' as seen in Fig. 5(b). Finally, the third stage will involve the thermal emission and the erbium excitation on a long time scale. After the first two stages, the system will be ''prepared'' in a quasis-

tationary (through nonequilibrium) state with no free carriers and equal concentration of charged impurities at donor and acceptor levels. Since (shallow) donor-acceptor recombination in Si must involve momentum compensation, it is an extremely slow process. In this way, the system can ''store'' nonequilibrium charges for a long time.

The MIR-induced Er PL is the best investigated under conditions of low excitation density.[13] In that case, we should not expect a band-to-band recombination and can assign $r=0$. During the short ($\sim$100 ps) duration of Nd:YAG excitation (Δt_{YAG}), we obtain: $n=p=\alpha\Delta t_{\mathrm{YAG}} I$. We can now find the expressions for f and f' from Eqs. (3) and (4),

$$f=\frac{C_{tr}}{C_{tr}+C_{ptr}}+\left(f_{00}-\frac{C_{tr}}{C_{tr}+C_{ptr}}\right)\times\exp[-(C_{tr}+C_{ptr})\alpha\Delta t_{\mathrm{YAG}} It], \tag{6}$$

$$f'=\frac{C_{d\mathrm{Er}}}{C_{d\mathrm{Er}}+C_A}+\left(f'_{00}-\frac{C_{d\mathrm{Er}}}{C_{d\mathrm{Er}}+C_A}\right)\times\exp[-(C_{d\mathrm{Er}}+C_A)\alpha\Delta t_{\mathrm{YAG}} It], \tag{7}$$

where f_{00} and f'_{00} are the values of the initial filling factors. After several intervals of $(\alpha\Delta t_{\mathrm{YAG}} I)^{-1}$ the filling factors will arrive at the limiting values depending only on the capture coefficients: $f=[C_{tr}/(C_{tr}+C_{ptr})]$ and $f'=[C_{d\mathrm{Er}}/(C_{d\mathrm{Er}}+C_A)]$. However, this is not yet the end of the second stage, since charges at donor and acceptor levels with these limiting filling factors are not equal. This means actually that there remain some free carriers in the conduction or valence band depending on the ratio of capture coefficients and concentration of impurities. The further capture of these free carriers will equalize the charge at donor and acceptor levels leading to the true limiting values of filling coefficients,

$$f=F_0=1-f'=1-F'_0=\frac{C_{tr}}{C_{tr}+C_{ptr}}\left[N_{tr}\frac{C_{d\mathrm{Er}}C_A}{C_{d\mathrm{Er}}+C_A}+N_{\mathrm{Er}}\frac{C_A C_{ptr}}{C_{d\mathrm{Er}}+C_A}\right]\left[N_{tr}\frac{C_{tr}C_{ptr}}{C_{tr}+C_{ptr}}+N_{\mathrm{Er}}\frac{C_{d\mathrm{Er}}C_A}{C_{d\mathrm{Er}}+C_A}\right]^{-1}. \tag{8}$$

At this point, considering linear regime of Er PL, some erbium ions are excited and decay with a lifetime of $\tau\approx 1$ ms. In the third stage, the system is prepared for the slow excitation mechanism, as can be seen in Fig. 5(c). After all the fast processes have finished, the recombination will be controlled by the thermal release of holes from traps into the valence band and their subsequent capture at erbium donor levels. We will neglect that there is a thermal emission of electrons from the Er-related donor level into the conduction band. This is reasonable, taking into account the postulated large ionization energy of this level $E_{\mathrm{Er}}\gtrsim 150$ meV and high concentration of Er in the implanted layer. The new rate equations for slow excitation are

$$\frac{dp}{dt}=-C_{ptr}pN_{tr}f-C_A pN_{\mathrm{Er}}f'+C_{ptr}p_0\frac{f_0}{(1-f_0)}N_{tr}(1-f), \tag{9}$$

$$N_{tr}\frac{df}{dt}=-C_{ptr}pN_{tr}f+C_{ptr}p_0\frac{f_0}{(1-f_0)}N_{tr}(1-f), \tag{10}$$

$$N_{\mathrm{Er}}\frac{df'}{dt}=-C_A pN_{\mathrm{Er}}f'. \tag{11}$$

It can be shown that due to slow thermal process of hole release from traps into the valence band, we can neglect the derivative in Eq. (9) and consider quasistationary conditions. The hole concentration can then be expressed by

$$p=\frac{C_{ptr}p_0 f_0}{(1-f_0)(C_A N_{\mathrm{Er}}F'_0+C_{ptr}N_{tr}F_0)}N_{tr}(1-f), \tag{12}$$

and inserting Eq. (12) into Eq. (10) we arrive at the solution

$$(1-f)=(1-F_0)\times\exp\left(-\frac{C_{ptr}p_0 f_0}{1-f_0}\frac{C_A N_{\mathrm{Er}}F'_0}{C_A N_{\mathrm{Er}}F'_0+C_{ptr}N_{tr}F_0}t\right). \tag{13}$$

The second factor under the exponent increases the characteristic time of slow recombination since the part of holes emitted into the band are captured again by hole traps. Using Eq. (13) in Eq. (12), the time-dependent expression for the hole concentration will be

$$p=\frac{C_{ptr}p_0 f_0 N_{tr}(1-F_0)}{(1-f_0)(C_A N_{\mathrm{Er}}F'_0+C_{ptr}N_{tr}F_0)}\times\exp\left(-\frac{C_{ptr}p_0 f_0}{1-f_0}\frac{C_A N_{\mathrm{Er}}F'_0}{C_A N_{\mathrm{Er}}F'_0+C_{ptr}N_{tr}F_0}t\right). \tag{14}$$

In this equation we neglect the first derivative since $[(C_{ptr}p_0 f_0)/(1-f_0)](C_A N_{\mathrm{Er}}F'_0+C_{ptr}N_{tr}F_0)^{-1}\ll 1$. Using the hole concentration given by Eq. (14) and substituting it into Eq. (11), we arrive at

$$f'=F'_0-\frac{N_{tr}}{N_{\mathrm{Er}}}(1-F_0)\times\left\{1-\exp\left(-\frac{C_{ptr}p_0 f_0}{1-f_0}\frac{C_A N_{\mathrm{Er}}F'_0}{C_A N_{\mathrm{Er}}F'_0+C_{ptr}N_{tr}F_0}t\right)\right\}. \tag{15}$$

This slow recombination process is characterized by a time constant of

$$\tau_{sr}=\left(\frac{C_{ptr}p_0 f_0}{1-f_0}\frac{C_A N_{\mathrm{Er}}F'_0}{C_A N_{\mathrm{Er}}F'_0+C_{ptr}N_{tr}F_0}\right)^{-1}, \tag{16}$$

and we can use Eq. (15) as the ''driving force'' for excitation. In order to solve Eq. (5), we assume that the slow Er^{3+} excitation can be considered as a quasistationary one. The result will be

$$N^* \approx C_A p f' N_{\mathrm{Er}} \tau \approx \left(\frac{\tau}{\tau_{sr}}\right) N_{tr}(1-F_0)\exp\left(-\frac{t}{\tau_{sr}}\right). \quad (17)$$

Due to the presence of $p_0 f_0$, the parameter τ_{sr} will contain an exponent: $\exp(-E_{trap}/kT)$, where E_{trap} is the binding energy of the hole trap (from the top of the valence band). At $T=4.2$ K, the slow excitation will be important but at higher temperatures ($T \approx 45$ K) it will disappear, as verified experimentally.[13]

2. MIR-induced Er PL enhancement

We will now consider what will happen when an intense MIR pulse is applied at $t=t_1$. The MIR radiation will liberate holes into the valence band and an abrupt increase of Er PL should be observed. This situation is depicted in Fig. 5(d). The relevant rate equations are

$$\frac{dp}{dt} = \beta I_{\mathrm{FEL}} \delta(t-t_1) N_{tr}(1-f) - C_{ptr} p N_{tr} f - C_A p N_{\mathrm{Er}} f', \quad (18)$$

$$N_{tr}\frac{df}{dt} = \beta I_{\mathrm{FEL}} \delta(t-t_1) N_{tr}(1-f) - C_{ptr} p N_{tr} f, \quad (19)$$

$$N_{\mathrm{Er}}\frac{df'}{dt} = -C_A p N_{\mathrm{Er}} f', \quad (20)$$

where β is the absorption coefficient of the FEL emission and I_{FEL} is the intensity of the FEL pulse fired at $t=t_1$. Again, we first consider the fast processes. In this case, we start by Eq. (19). During FEL pulse (Δt_{FEL}), we have

$$f = f_{01} + (1-f_{01})\{1-\exp(-\beta I_{\mathrm{FEL}} \Delta t_{\mathrm{FEL}})\}, \quad (21)$$

where $f_{01}=1-(1-F_0)\exp(-t_1/\tau_{sr})$ is the filling factor at time $t=t_1$ taken from Eq. (13). Using a similar value for f'_{01} obtained from Eq. (14), we can solve Eq. (18) during FEL pulse. In a linear approximation, we get

$$p = \frac{\beta I_{\mathrm{FEL}} N_{tr}(1-f_{01})}{C_{ptr}N_{tr}f_{01} + C_A N_{\mathrm{Er}} f'_{01}} \times \{1-\exp[-(C_{ptr}N_{tr}f_{01} + C_A N_{\mathrm{Er}} f'_{01})t]\}. \quad (22)$$

Upon termination of the FEL pulse the concentration of holes will diminish exponentially,

$$p = p_{00}\{1-\exp[-(C_{ptr}N_{tr}f_{02} + C_A N_{\mathrm{Er}} f'_{01})t]\}, \quad (23)$$

where p_{00} is the concentration of holes given by Eq. (22) for $t=\Delta t_{\mathrm{FEL}}$ and f_{02} is the filling factor as given by Eq. (21) at the end of FEL pulse for $t=t_2$, $\Delta t_{\mathrm{FEL}}=(t_2-t_1)$. Substituting this solution into Eq. (20) we obtain

$$f' = f'_{01} - \frac{C_A f'_{01} p_{00}}{(C_{ptr}N_{tr}f_{02} + C_A N_{\mathrm{Er}} f'_{01})} \times \{1-\exp[-(C_{ptr}N_{tr}f_{02} + C_A N_{\mathrm{Er}} f'_{01})t]\}, \quad (24)$$

and a similar expression for f. After the recharging induced by FEL, the filling factors will arrive at the limiting values: F'_{01} following from Eq. (24) and F_{01} from the one related to f. These limiting values ensure the neutrality condition of charge equality at donors and acceptors. Later on, these factors will change according to the slow recombination τ_{sr} process described in the preceding subsection. In order to study the dynamics of N^*, we consider that an abrupt increase of $p \approx p_{00}$ in a delta-shape pulse, is responsible for the erbium excitation. In this case the concentration of erbium after solving Eq. (5) will be

$$N^* = N^*_{00} + \left[\frac{C_A p_{00} f'_{01} N_{\mathrm{Er}}}{C_A p_{00} f'_{01} + \tau^{-1}} - N^*_{00}\right]\{1-\exp(-C_A p_{00} f'_{01} t)\}, \quad (25)$$

where $N^*_{00} = N_{tr}(\tau/\tau_{sr})(1-F_0)\exp(-t_1/\tau_{sr})$ is the concentration of excited erbium ions at the moment when FEL is switched on. Since the traps during FEL pulse loose holes, the slow excitation value of N^* will drop to a value of N^*_{01}. The concentration of excited erbium ions, and thus also the intensity of Er-related PL after FEL pulse, will evolve the following expression:

$$I_{\mathrm{PL}} \sim N^* = N^*_{00} + \left[\frac{C_A p_{00} f'_{01} N_{\mathrm{Er}}}{C_A p_{00} f'_{01} + \tau^{-1}} - N^*_{00}\right] \times \{1-\exp(-C_A p_{00} f'_{01} \Delta t_{\mathrm{FEL}})\}\exp\left(-\frac{(t-t_1)}{\tau}\right) + N^*_{01}\left\{1-\exp\left(-\frac{(t-t_1)}{\tau}\right)\right\}\exp\left(-\frac{(t-t_1)}{\tau_{sr}}\right), \quad (26)$$

where

$$N^*_{01} = \frac{C_{ptr}p_0 f_0}{1-f_0}\frac{C_A N_{\mathrm{Er}} F'_{01}}{C_{ptr}N_{tr}F_{01} + C_A N_{\mathrm{Er}} F'_{01}} N_{tr}(1-F_{01})\tau \times \exp\left(-\frac{C_{ptr}p_0 f_0}{1-f_0}\frac{C_A N_{\mathrm{Er}} F'_0}{C_{ptr}N_{tr}F_0 + C_A N_{\mathrm{Er}} F'_0} t_1\right).$$

Expression (26) agrees well with the experimental results allowing to reproduce the slow afterglow effect, and its reduction following the MIR-induced enhancement.[13] In the above description the response time of the detector is not considered, but that will influence only the rising time of the (FEL-induced) Er PL signal which will become slower. In this model, the sublinear dependence of the enhancement effect—see Fig. 2—is explained. The MIR radiation only release one type of carrier so that the effect is proportional to I_{FEL}. The saturation term is actually connected to the filling factor of hole traps and not to the saturation of erbium. It can be also shown that if the capture probability of holes by traps

is higher than by Er-related donors, the majority of holes induced by Nd:YAG are captured and stored at the traps. In this case, the intensity of the erbium PL induced by MIR radiation can significantly exceed that of the initial pulse, as confirmed experimentally.

C. Comparison with experiment

The system of Eqs. (1)–(5) contains many constants which should be taken from experiment for simulation of results. Therefore, the simulation procedure is rather cumbersome and subjected to some arbitrariness. Besides, the measurements of power dependence of luminescence intensity were done in arbitrary units, since accurate measurements of absolute intensities are difficult. This fact does not allow to determine parameters of the material (for instance, the concentration of traps) directly from the experimental data shown in Figs. 2 and 3. However, it is easy to obtain approximate solutions of a simplified system of the rate equations and compare the resulting functional power dependences of luminescence intensity with the experiment. These solutions concern with the dependence of the Er PL intensity on the power of the Nd:YAG laser (initial excitation) and the dependence of the Er PL enhancement on the power of FEL (delayed excitation).

If the characteristic capture times are small compared to the duration of both laser pulses, we can use the quasistationary approximation for the state during the laser pulse. We shall use the linearized version of rate equations assuming that the intensity of initial PL signal excited by the yttrium aluminum garnet (YAG) laser is proportional to the concentration of free holes, while that of the delayed PL signal induced by FEL to the concentration of holes bound at the traps. This assumption suggests that the necessary concentration of electrons for the excitation Auger process is always available (they can be in the conduction band during the Nd:YAG pulse or populate the donor levels).

If this concentration of electrons does not change significantly during the Nd:YAG laser pulse, the calculated concentration of free (or bound) holes reflects the amplitude of the PL signal measured in arbitrary units, i.e., the calculations of the hole concentrations can be directly compared to the experiment represented in Figs. 2 and 3.

To consider the dependence of the PL enhancement on the FEL power, we can use one equation for free holes in the form

$$\frac{dp}{dt}=\beta_0 I_{\mathrm{FEL}}(N_{tr}-p)-C_{ptr}p^2=0, \tag{27}$$

where we have used the condition that the concentration of free holes in the case of excitation from the traps should be equal to the concentration of the trap states without holes, i.e., filled by electrons. The solution of this quadratic equation is fitted to experimental data in Fig. 2, demonstrating a fair agreement. At low FEL powers, the PL intensity grows as a square root and then tends to saturation.

To determine the dependence of the Er emission on the YAG power we need the system of equations

$$\frac{dp}{dt}=\alpha I_{\mathrm{YAG}}-C_{ptr}p(N_{tr}-p_b)-\frac{p}{\tau_p}=0, \tag{28}$$

$$\frac{dp_b}{dt}=C_{ptr}p(N_{tr}-p_b)-\frac{p_b}{\tau_b}=0. \tag{29}$$

We have introduced here the concentration of bound holes p_b instead of the population factor of the trap states [$p_b=N_{tr}(1-f)$], and two characteristic lifetimes of free and bound holes which are connected with the capture coefficients and some concentration of electrons in the conduction band which is assumed constant for the purpose of linearization of the equations involved ($\tau_p^{-1}=rn, \tau_b^{-1}=C_{tr}n$). This means that our approximation is fairly crude; nevertheless, it gives a good agreement with the experiment.

The solution of this system connects directly the behavior of initial and delayed PL signals: until all the traps are not filled, the initial PL signal rises weakly with the Nd:YAG intensity, and only when the saturation of the delayed PL is reached, this rise becomes stronger. The simulation of experimental results according to the solution of Eqs. (28)–(29) is compared in Fig. 3 with the measured amplitude of Nd:YAG- and FEL-induced Er PL signals demonstrating a good correspondence between the experiment and the theory.

Finally, we should present numerical values of relevant parameters which permit the use of quasistationary approximation and allow the satisfactory simulation of experimental data. To support the approximation of quasistationary situation it is necessary to estimate the capture times. The following values of these parameters were adopted: the concentration of traps $N_{tr}=10^{15}$ cm^{-3}, the capture coefficient of holes $C_{ptr}=\sigma_h V_h$, where the capture cross section of holes by negatively charged center $\sigma_h=10^{-10}$ cm^2,[16] $V_h \approx 10^6$ cm s^{-1} is the hole velocity, so the capture time is much less than the duration of the YAG (and FEL) pulse. The capture coefficient of the electrons by a neutral acceptor center is $C_{tr}=\sigma_e V_e$, $\sigma_e=10^{-16}$ cm^2,[16] $V_e \approx 10^6$ cm s^{-1}, and the capture time is of the order of the pulse of Nd:YAG duration. The recombination time τ_p can be estimated from the data of Thao *et al.*,[17] where the value of nonradiative recombination coefficient at low temperature of the order of 10^{-10} cm^3 s^{-1} is given. Therefore, the characteristic lifetime is around 4×10^{-10} s for the YAG photon flux of 10^{24} cm^{-2} s^{-1} using the absorption coefficient value of 4×10^4 cm^{-1} (in this case the concentration induced by YAG is 2.3×10^{19} cm^{-3}). The reasonable value of absorption cross-section β_0 for the FEL radiation is 10^{-16} cm^2, so the absorption coefficient can be 0.1. The photon fluxes of the YAG laser is of the order of 10^{24} cm^{-2} s^{-1}, while that of FEL is 2×10^{19} cm^{-2} s^{-1}. We note that these estimates are consistent with the quasistationary approximation used in the model and justify the use of quasistationary solutions.

V. DEVICE IMPLICATIONS

There are two important conditions which have to be satisfied in order to develop Si:Er-based devices for room-temperature operation. We need efficient excitation of Er

ions while at the same time nonradiative deexcitation should have to be suppressed. Excitonic process provides a good excitation of Er at low temperatures. Unfortunately, its efficiency diminishes upon temperature increase due to dissociation of excitons. Yet another problem, appearing for higher temperatures and for high pumping densities, is the Auger energy transfer to free carriers. This nonradiative recombination limits the maximum number of Er^{3+} ions that can attain the excited state. Our current results offer a possibility to circumvent this problem. As discussed in the previous sections, excitation of Er^{3+} ions can be realized by the recombination of electrons localized at the Er-related level shortly after band-to-band excitation with holes supplied subsequently by (thermal or optical) the ionization of traps. The most characteristic feature of this process is the time separation of electron capture and the electron-hole recombination. Consequently, the erbium excitation is effectively governed only by the release of holes into the band. In this case Er^{3+} ions are prepared for excitation by capturing of electrons at the Er-related level. Since our research shows that processes of electron capture and electron-hole recombination can be arbitrarily separated in time, the preparation of the Si:Er system for excitation is realized by filling all the Er-related electron traps—a condition easily fulfilled in *n*-type material. The excitation can then be accomplished upon injection of holes. In such a scheme, the free carrier concentration can be much lower than that required for efficient exciton generation. Consequently, the Auger deexcitation would be suppressed. Exploration of this excitation route could open new possibilities for efficient reduction of thermal quenching of emission from Si:Er structures.

A separate issue is the question of whether the MIR-induced generation of Er PL could be realized also at a higher (and possibly room) temperature. According to our model, τ_{sr} relates to thermal release of holes into the band and, as such, it is directly related to the ionization energy of the trap. In our experiments we have used *p*-type boron-doped Si substrates, so the holes were trapped at shallow acceptors. Naturally, shallow traps thermalize above $T \gtrsim 45$ K and the MIR-induced Er PL vanishes. In the presence of deep acceptors, however, we can expect a longer value of τ_{sr} and the enhancement effect could take place at higher temperatures. Possible candidate impurities for deeper acceptor traps could be, e.g., indium (single acceptor at 155 meV above the valence band) or a double acceptor zinc. We note that thermalization of the Er-related electron trap is of lesser importance in view of the high Er concentration in the implanted layer, which compensates the statistical advantage of the band.

VI. CONCLUSIONS

A nonexcitonic mechanism of 1.54 μm emission of Er^{3+} ions in a crystalline silicon has been identified and microscopically modeled. Excitation of Er^{3+} is achieved upon the release of free holes into the band, by their recombination with electrons localized at Er-related donors. Therefore, this mechanism is most pronounced for comparable concentrations of donors and acceptors. In samples prepared from *p*-type substrates, the nonexcitonic mechanism dominates under low pumping rates and is also responsible for the recently reported low-temperature effects of afterglow and the MIR-induced Er PL. The essential feature of the newly identified Er excitation channel is the stable character of the situation when electrons are captured at the Er-related traps. In this state, which can persist indefinitely, the Si:Er system is prepared for excitation which then takes place at an arbitrary moment, upon arrival of holes. This finding could open new ways towards the increase of thermal stability of PL emission from Si:Er. Also, in contrast to the exciton-mediated mechanism, the discussed excitation path does not require high concentrations of free carriers (electron and holes can be introduced at different time intervals). This limits the Auger quenching of excited Er^{3+} ions which appears at low temperatures for high pumping rates.

ACKNOWLEDGMENTS

We acknowledge W. Jantsch and A. Polman for providing Si:Er material used in this study. This work was financially supported by the *European Research Office* (ERO) and the *Stichting voor Fundamenteel Onderzoek der Materie* (FOM). The work of M.S.B. and O.B.G. was partially funded by Nederlandse Organisatie voor Wetenschappelijk Onderzoek (NWO), and grants from Russian Foundation of Basic Research (Grant No. 02-02-17631) and from Russian Ministry of Science and Technology.

[1] L. Pavesi, L. Dal Negro, G. Franzò, and F. Priolo, Nature (London) **408**, 440 (2000).

[2] K. Watanabe, S. Takeoka, M. Fujii, S. Hayashi, and K. Yamamoto, J. Lumin. **87-89**, 426 (2000).

[3] Wai Lek Ng, M.A. Lourenço, R.M. Gwilliam, S. Ledain, G. Shao, and K.P. Homewood, Nature (London) **410**, 192 (2001).

[4] I.N. Yassievich and L.C. Kimerling, Semicond. Sci. Technol. **8**, 718 (1993).

[5] G.N. van den Hoven, Jung H. Shin, A. Polman, S. Lombardo, and S.U. Campisano, J. Appl. Phys. **78**, 2642 (1995).

[6] F. Priolo, G. Franzò, S. Coffa, and A. Carnera, Phys. Rev. B **57**, 4443 (1998).

[7] J. Palm, F. Gan, B. Zheng, J. Michel, and L.C. Kimerling, Phys. Rev. B **54**, 17 603 (1996).

[8] O.B. Gusev, M.S. Bresler, P.E. Pak, I.N. Yassievich, M. Forcales, N.Q. Vinh, and T. Gregorkiewicz, Phys. Rev. B **64**, 075302 (2001).

[9] M.S. Bresler, O.B. Gusev, B.P. Zakharchenya, and I.N. Yassievich, Phys. Solid State **38**, 813 (1996).

[10] M. Forcales, M. Klik, N.Q. Vinh, I.V. Bradley, J-P.R. Wells, and T. Gregorkiewicz, J. Lumin. **94**, 243 (2001).

[11] T. Gregorkiewicz, D.T.X. Thao, and J.M. Langer, Appl. Phys. Lett. **75**, 4121 (1999).

[12] T. Gregorkiewicz, D.T.X. Thao, J.M. Langer, H.H.H.Th. Bekman,

M.S. Bresler, J. Michel, and L.C. Kimerling, Phys. Rev. B **61**, 5369 (2000).
[13] M. Forcales, T. Gregorkiewicz, I.V. Bradley, and J-P.R. Wells, Phys. Rev. B **65**, 195208 (2002).
[14] F.P. Widdershoven and J.P.M. Naus, Mater. Sci. Eng., B **B4**, 71 (1989)
[15] S. Libertino, S. Coffa, G. Franzò, and F. Priolo, J. Appl. Phys. **78**, 3867 (1995).
[16] V. N. Abakumov, V. I. Perel, and I. N. Yassievich, *Nonradiative Recombination in Semiconductors*, edited by V. N. Abakumov and A. A. Maradudin (North-Holland, Amsterdam, 1991), Vol. 33.
[17] D.T.X. Thao, C.A.J. Ammerlaan, and T. Gregorkiewicz, J. Appl. Phys. **88**, 1443 (2000).